This article has been accepted for publication in a future issue of this journal, but has not been fully edited. Content may change prior to final publication. Citation information: DOI 10.1109/TCOMM.2014.2334619, IEEE Transactions on Communications

A New MSE Channel Estimator Optimized for Nonlinearly Distorted Faded OFDM Signals with Applications to Radio-over-Fiber

João M. B. Oliveira, Henrique M. Salgado, *Member, IEEE*, and Miguel R. D. Rodrigues, *Member, IEEE,*

***Abstract*—In this paper, we propose a new channel estimation (CE) structure that aims to minimize the mean-squared error (MMSE) of orthogonal frequency division multiplexing (OFDM) signals that are corrupted by fading, nonlinear and additive white Gaussian noise channels. We demonstrate that it exhibits a simple structure consisting of a set of correlators matched to every frequency component in the nonlinearly distorted signal, followed by a linear transformation. An extension suitable for frequency shifted signals is also discussed.**

As case study, the potential of such CE in uplink radio-over-fiber (RoF) systems conveying WiFi signals is analyzed. Through simulations, we demonstrate the usage of the one-tap and an iterative maximum likelihood (ML) algorithm based equalizers, when used jointly with the proposed MMSE, zero forcing (ZF) or perfect CEs. Results show that the performance of the MMSE CE approximates the one of the perfect CE. Also, when used in conjunction with the ML algorithm it enables relaxation of linear requirements of components in RoF by passing the need for transmitter pre-distortion techniques that would otherwise increase significantly wireless devices complexity.

***Index Terms*—OFDM, fading, mean square error methods, optical fiber communication, nonlinear distortion, maximum likelihood detection.**

This work was partly funded by FP7 project Daphne, grant ACP8-GA-2009-233709, by the ERDF through COMPETE Programme and by the FCT within project FCOMP-01-0124-FEDER-022701 and Programme POCTI/FEDER with grant REEQ/1272/EEI/2005. Project "NORTE-07-0124-FEDER-000058" is financed by the North Portugal Regional Operational Programme (ON.2 O Novo Norte), under the National Strategic Reference Framework (NSRF), through the European Regional Development Fund (ERDF), and by national funds, through the Portuguese funding agency, Fundação para a Ciência e a Tecnologia (FCT).

João M. B. Oliveira is with Synopsys Inc., Portugal (email: joao.oliveira@synopsys.com).

Henrique M. Salgado is with INESC TEC - INESC Technology and Science (formerly INESC Porto), Porto, Portugal, and with Faculty of Engineering, University of Porto, Portugal (e-mail: henrique.salgado@inescporto.pt).

Miguel R. D. Rodrigues is with the Department of Electronic and Electrical Engineering, University College London, London, UK (e-mail: m.rodrigues@ucl.ac.uk).

I. Introduction

It is true that the demand for broadband contents and services in both wired and wireless technologies has been growing rapidly. We are living in an era where broadband Internet with high bandwidth services and applications such as HD multimedia, real-time video, fast P2P and on-line gaming are continuously evolving and demanding for even higher data rates. The residential home market has also grown tremendously in the past few years leading to an increase in the number of wireless access subscribers calling for higher bandwidths (e.g. [1], [2]).

An interesting recent phenomenon relates to the increase in the uplink data traffic. This phenomenon is mainly due to the exponential use of Internet services like social networks and video/photo sharing combined with the ever increasing mobile systems with full-HD capabilities and high speed connectivity. Therefore, it is clear that wireless standards will have to be able to provide both broadband downlink and uplink solutions. A notable scheme that is the basis for the realization of such broadband downlink and uplink solutions is orthogonal frequency division multiplexing (OFDM). In addition, due to its good performance in multipath fading environments without the need of complex equalization processes, OFDM offers many advantages including high spectral efficiency and FFT based efficient DSP transceiver implementations [3]. These characteristics make it the preferred scheme for current and modern wireless standards like, e.g, Wi-Fi IEEE 802.11a/g/n [4], [5] and WiMAX IEEE 802.16/e [6]. Yet, due to its multicarrier nature, OFDM is very sensitive to frequency, clock and phase offsets and also exhibits a high peak-to-average ratio (PAPR), which leads to a high

This article has been accepted for publication in a future issue of this journal, but has not been fully edited. Content may change prior to final publication. Citation information: DOI 10.1109/TCOMM.2014.2334619, IEEE Transactions on Communications

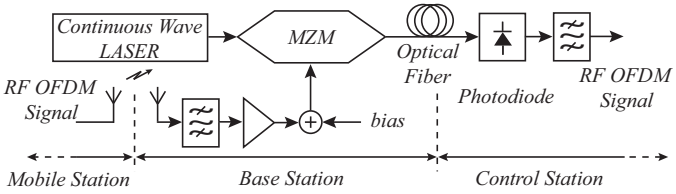

Fig. 1. Representation of an uplink radio-over-fiber system.

sensitivity to nonlinear distortion.

To reduce system cost, maintenance and complexity in upcoming dense cell based wireless systems [2], which will play a prominent role in enabling future wireless, it is important to simplify antenna units or base stations (BS) and to concentrate signal processing functions at a centralized headend, usually referred to as the central station (CS). In particular, there is currently a considerable widespread interest in using radio-over-fiber (RoF) techniques to transport and deliver RF signals from BS to the CS, including wireless OFDM based standards. The RoF concept is based on the modulation of an optical carrier by an RF signal so that it can be distributed over an optical fiber based network. A generic RoF system is composed by a CS and several BS designed only for wireless signal distribution. By using the optical fiber as the transport medium, we are taking advantage of low loss and high bandwidth transmission. Its architecture permits significantly simple BSs since they usually only perform optical-electrical-optical (O/E/O) conversion and, in some cases, filter and amplification operations. Additionally, the expensive high frequency equipment can be shared and concentrated at the CS, which enables future upgrade tasks easier and system installation and maintenance cost savings [7]. Nevertheless, these systems also suffer from specific impairments which include the nonlinearities associated with various optical components such as E/O converters. This type of impairment is particularly problematic for OFDM signals, so efficient techniques are on demand to counteract the nonlinear phenomena.

In this paper, we focus on RoF uplink wireless transmission systems that leverage post-compensation rather than pre-distortion techniques in order to limit the complexity of the mobile device. Specifically, we consider an uplink intensity modulation/direct detection (IM/DD) RoF system based on external modulation of a LASER by means of a Mach-Zehnder modulator (MZM) (see Figure 1). Due to the effect of both the wireless channel and the MZM, the signal is linearly and nonlinearly distorted, respectively. Specifically, the nonlinearity causes intermodulation distortion (IMD) to arise and to fall both inside and outside the signal's band, causing error penalty and signal spectral spreading. Additionally, IMD also limits considerably the performance of any channel estimation process.

Since linear MMSE based techniques (e.g. [8]–[12]) that only exploit the behavior of the linear portion of the channel are unlikely to perform well in the presence of nonlinear distortion, the goal of this work is to derive linear CEs that embody both the effect of the linear and nonlinear components of the communications channel usually present in RoF uplink systems. It is also important to highlight that it is a topic that is not well exploited in the literature. In particular, we derive the structure of the MMSE CE for faded OFDM signals distorted by a bandpass nonlinearity and AWGN. We demonstrate that it consists of a set of correlators or a set of filters matched to every possible frequency components in the nonlinearly distorted OFDM signal followed by a linear transformation. It is shown that this structure outperforms conventional zero forcing (ZF) CEs and to perform similarly to perfect CE.

This paper is organized as follows: Section II introduces the system model under study; Section III derives the proposed MMSE channel estimator structure; Section IV compares the performances of the ZF, MMSE and perfect CE with both one-tap and ML algorithm equalizers for OFDM signals based on IEEE802.11g/n conveyed by a RoF system; Finally, Section V summarizes the main contributions and their implications for RoF based wireless systems design.

II. System model

The equivalent baseband OFDM communications system in Figure 2 represents an abstraction of the OFDM RoF uplink system in Figure 1, where the bandpass fading channel corresponds to the radio channel between the remote antenna unit and the wireless device, the bandpass nonlinearity is caused by the electro-optic modulator and the AWGN source is caused by the combined photodiode thermal and shot noises and receiver thermal noise. We now describe the main system blocks in detail.

This article has been accepted for publication in a future issue of this journal, but has not been fully edited. Content may change prior to final publication. Citation information: DOI 10.1109/TCOMM.2014.2334619, IEEE Transactions on Communications

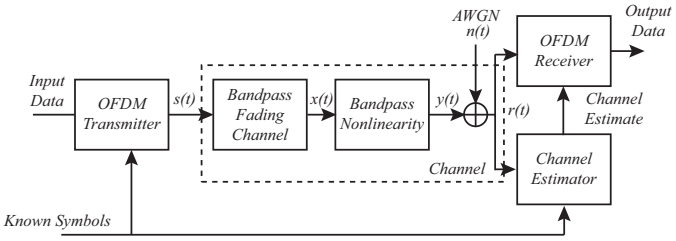

Fig. 2. Equivalent baseband uplink wireless communication model.

A. OFDM transmitter

The complex envelope of the transmitted bandpass OFDM signal is given by [3]

$$s(t) = \sum_{k=-\infty}^{\infty} \sum_{n=0}^{N-1} S_{k,n} g_n(t - kT) \tag{1}$$

and

$$g_n(t) = \begin{cases} \dfrac{1}{\sqrt{T - T_{CP}}} e^{j\frac{2\pi n(t-T_{CP})}{T-T_{CP}}}, & 0 \le t \le T \\ 0, & \text{otherwise,} \end{cases} \tag{2}$$

where $S_{k,n}$ is the complex transmitted symbol in time slot k and subchannel n, T is the total OFDM symbol duration, N is the number of OFDM subcarriers and T_{CP} is the cyclic prefix duration. The complex symbols conveyed by different time slots and subcarrier are assumed to be statistically independent and to follow a constellation scheme of size M[1].

B. Channel

The complex envelope of the received OFDM signal is given by

$$r(t) = y(t) + n(t) = f(s(t) * h(t)) + n(t) \tag{3}$$

where $h(t)$ is the complex impulse response (IR) of the bandpass fading channel, $y(t)$ is the complex envelope of the nonlinearly distorted faded signal, $n(t)$ is the complex envelope of bandpass AWGN and $f(\cdot)$ denotes the input-output characteristic of the nonlinearity considered to be given by a complex Taylor series [13]

$$f\left(x(t)\right) = \sum_{i=1}^{\infty} c_{2i-1} x(t) |x(t)|^{2i-2} \tag{4}$$

[1]Note that independence assumptions are typically valid for uncoded transmissions as well as coded transmission that use interleavers/de-interleavers to uncorrelate the data. Thus, this assumption does not entail significant loss in generality.

with complex coefficients c_l. Note that this approach offers a simple way to describe a nonlinearity, allowing us to directly obtain the harmonic levels in terms of the expansion coefficients. The lowpass equivalent representation of the IR of the multipath channel is considered to be given by (e.g. [3], [14])

$$h(t) = \sum_{g=0}^{G-1} h_g \delta^D(t - t_g) \tag{5}$$

where h_g and t_g are the different path complex gains/attenuations and time delays, respectively, G is the total number of paths and $\delta^D(\cdot)$ is the Dirac delta function. We take the channel coherence time to be much longer than the OFDM symbol duration, which typically occurs in various scenarios of practical relevance [3], [14]. The corresponding channel transfer function, $H(f)$, is given by its Fourier transform. In typical tapped delay line (TDL) models akin to (5) it is common to assume that h_g follow a zero-mean circularly symmetric complex Gaussian distribution for Rayleigh fading models, or a nonzero-mean, for Ricean fading models. The exact gains are dictated by the power delay profile (PDP) that is typically taken to decay exponentially in time [15].

C. OFDM receiver

The structure of the conventional OFDM receiver can be viewed as a set of N correlators matched to the various subcarriers frequencies, i.e.,

$$R_{k,n} = \int_{kT+T_{CP}}^{(k+1)T} r(t) g_n^*(t - kT) dt \tag{6}$$

We assume that T_{CP} is longer than the duration of the channel IR. Then, by using (3) in (6) it is possible to express the received symbol as follows

$$\begin{aligned} R_{k,n} &= Y_{k,n} + N_{k,n} \\ &= \sum_{i=1}^{\infty} \frac{c_{2i-1}}{(T - T_{CP})^{i-1}} \sum_{n_1=0}^{N-1} \cdots \sum_{n_{2i-1}=0}^{N-1} S_{k,n_1} H_{k,n_1} \cdots \\ &\cdots S_{k,n_i} H_{k,n_i} S^*_{k,n_{i+1}} H^*_{k,n_{i+1}} \cdots S^*_{k,n_{2i-1}} H^*_{k,n_{2i-1}} \\ &\times \delta(n_1 + \cdots + n_i - n_{i+1} - \cdots - n_{2i-1} - n) + N_{k,n} \end{aligned} \tag{7}$$

where $\delta(\cdot)$ represents the Kronecker delta function, $H_{k,n} = H(n/(kT))$ represents the frequency response of the bandpass fading channel in time slot k and subchannel n and $N_{k,n}$ represents a circularly

This article has been accepted for publication in a future issue of this journal, but has not been fully edited. Content may change prior to final publication. Citation information: DOI 10.1109/TCOMM.2014.2334619, IEEE Transactions on Communications

symmetric complex Gaussian noise random variable (RV). The symbol $Y_{k,n}$ is composed by both linearly and nonlinearly distorted terms. The latter are responsible for the appearance of intermodulation products (IMP) and, consequently, IMD.

We consider structures with two different equalizations: the one-tap and the ML algorithm. With the availability of an estimate of the multipath channel frequency response, $\hat{H}_{k,n}$, the one-tap equalizer OFDM receiver produces the estimate

$$\hat{S}_{k,n}^{1T} = \frac{R_{k,n}}{\hat{H}_{k,n}} = \frac{Y_{k,n}}{\hat{H}_{k,n}} + \frac{N_{k,n}}{\hat{H}_{k,n}} \tag{8}$$

Note that for high levels of nonlinear distortion the term $Y_{k,n}$ has a relatively low mean due to the compression factor and a high variance. Thus, depending on the magnitude of $\hat{H}_{k,n}$, the IMD may be enhanced by this equalization procedure. Alternatively, the ML estimate vector is given by

$$\hat{\mathbf{S}}_k^{ML} = \arg\max_{\mathbf{S}_k \in \mathcal{S}} L\left(\mathbf{R}_k \middle| \mathbf{S}_k, \hat{\mathbf{H}}_k\right) \tag{9}$$

where $\mathcal{S}$ represents the search space composed by M^N different possible symbol combinations, $\hat{\mathbf{H}}_k = [\hat{H}_{k,0}, \cdots, \hat{H}_{k,N-1}]$, $\mathbf{R}_k = [R_{k,0}, \cdots, R_{k,N-1}]$, $\mathbf{S}_k = [S_{k,0}, \cdots, S_{k,N-1}]$, $\hat{\mathbf{S}}_k^{ML} = [\hat{S}_{k,0}^{ML}, \cdots, \hat{S}_{k,N-1}^{ML}]$ and $L(\cdot)$ is the likelihood function [16].

D. A note on ZF channel estimation

In order to correctly estimate the transmited complex symbols, it is necessary to obtain an estimate of the fading channel. Conventional estimation methods are based on the transmission of known symbols at specific subcarrier indexes (pilots) (e.g., [3]). In the ZF channel estimation, the frequency response of the channel is obtained as follows

$$\hat{H}_{k,n_p}^{ZF} = \frac{R_{k,n_p}}{S_{k,n_p}} = \frac{Y_{k,n_p}}{S_{k,n_p}} + \frac{N_{k,n_p}}{S_{k,n_p}} \tag{10}$$

where the index n_p indicates the index of the pilot-subcarriers. In the presence of IMD, the performance of the ZF is severely affected since Y_{k,n_p} is extremely corrupted. Additionally, the noise term may suffer amplification.

III. The linear MMSE channel estimator

We now derive the new linear CE structure that processes the nonlinearly distorted OFDM signal corrupted by AWGN in order to optimize a performance metric, namely the MSE[2].

Our MMSE CE is a block-type pilot-aided channel estimation technique where a specific OFDM symbol is used in the estimation process of the frequency response of the multipath channel. Contrary to what happens with the ZF estimator and others MMSE estimators optimized for systems exhibiting linear distortion only, our approach does not disregard the potentially significant correlation between the information conveyed by different subcarriers due to nonlinear distortion. Additionally, it is assumed that both the input-output characteristic of the nonlinear channel and the statistical properties of the multipath channel are known by the estimator.

We take the estimator to consist of a set of N linear filters with IRs $u_n(t)$, $n = 0, 1, \cdots, N-1$, that produces estimates of the frequency response of the multipath channel associated with time slot k and subcarrier n given by

$$\hat{H}_{k,n} = \left[r^p(t) * u_n(t)\right]_{t=t_k} \triangleq \int_{-\infty}^{+\infty} u_n(\tau) r^p(t_k - \tau) d\tau \tag{11}$$

where $r^p(t)$ represents the complex envelope of the received OFDM signal given that the vector of pilot complex symbols $\mathbf{S}^p = [S_0^p, \cdots, S_{N-1}^p]^T$ was transmitted and $t_k = t_0 + kT$ is the sampling time instant, where t_0 is a constant time delay.

By leveraging the fact that the noise is white with PSD N_0, the MSE is given by

$$\begin{aligned}
\text{MSE} &= \mathrm{E}\left[\left\|\mathbf{H}_k - \hat{\mathbf{H}}_k\right\|^2 \middle| \mathbf{S}^p\right] \\
&= \sum_{n=0}^{N-1} \mathrm{E}\left[|H_{k,n}|^2\right] + 2N_0 \int u_n(\tau_1) u_n^*(\tau_1) d\tau_1 \\
&+ \iint u_n(\tau_1) u_n^*(\tau_2) \mathrm{E}\left[y^p(t_k - \tau_1) y^{p*}(t_k - \tau_2)\right] d\tau_1 d\tau_2 \\
&- \int u_n(\tau_1) \mathrm{E}\left[H_{k,n}^* y^p(t_k - \tau_1)\right] d\tau_1 \\
&- \int u_n^*(\tau_2) \mathrm{E}\left[H_{k,n} y^{p*}(t_k - \tau_2)\right] d\tau_2
\end{aligned} \tag{12}$$

where $\mathbf{H}_k = [H_{k,0}, H_{k,1}, \cdots, H_{k,N-1}]^T$ and $y^p(t)$ represents the complex envelope of the nonlinearly

[2]A nonlinear estimator would be, in principle, more efficient. Since its computational complexity is likely to be much higher than that of a linear estimator, we focus on the linear one only.

This article has been accepted for publication in a future issue of this journal, but has not been fully edited. Content may change prior to final publication. Citation information: DOI 10.1109/TCOMM.2014.2334619, IEEE Transactions on Communications

distorted OFDM signal given that the vector of pilot symbols $\mathbf{S}^p$ was transmitted.

The aim is to determine $u_n(t)$ that minimize the MSE. Using calculus of variations [17] it is possible to show that the optimal linear filter responses satisfy the set of integral equations

$$\int u_n(\tau')\mathrm{E}\left[y^{p*}(t_k-\tau)y^p(t_k-\tau')\right]d\tau' + 2N_0u_n(\tau) = \mathrm{E}\left[H_{k,n}y^{p*}(t_k-\tau)\right] \quad (13)$$

The filter IR can now be derived by computing the expected value and the integral in the right-hand side (RHS) and left-hand side (LHS), respectively, of (13). By using (3) and (4) and assuming that the nonlinearity exhibits nonlinear behaviour of maximum order L, the expected value in the RHS of (13) can be written as

$$\begin{aligned}&\mathrm{E}\left[H_{k,n}y^{p*}(t_k-t)\right] = \\ &= \sum_{i=1}^{(L+1)/2}\frac{c_{2i-1}^*}{(T-T_{CP})^{(i-1)/2}}\sum_{n_1=0}^{N-1}\cdots\sum_{n_{2i-1}=0}^{N-1} \\ &\times S_{n_1}^{p*}\cdots S_{n_i}^{p*}S_{n_{i+1}}^{p}\cdots S_{n_{2i-1}}^{p} \\ &\times \mathrm{E}\left[H_{k,n}H_{k,n_1}^*\cdots H_{k,n_i}^*H_{k,n_{i+1}}\cdots H_{k,n_{2i-1}}\right] \\ &\times g_{n_1+\cdots+n_i-n_{i+1}-\cdots-n_{2i-1}}^*(t_0-t)\end{aligned} \quad (14)$$

and the integral of the expected value in the LHS of (13) can be written as

$$\begin{aligned}&\int u_n(\tau')\mathrm{E}\left[y^{p*}(t_k-\tau)y^p(t_k-\tau')\right]d\tau' = \\ &= \sum_{i=1}^{(L+1)/2}\sum_{j=1}^{(L+1)/2}\frac{c_ic_j^*}{(T-T_{CP})^{(i+j-2)/2}} \\ &\times\sum_{n_1=0}^{N-1}\cdots\sum_{n_{2i-1}=0}^{N-1}\sum_{m_1=0}^{N-1}\cdots\sum_{m_{2i-1}=0}^{N-1}S_{n_1}^p\cdots S_{n_i}^p \\ &\times S_{n_{i+1}}^{p*}\cdots S_{n_{2i-1}}^{p*}S_{m_1}^{p*}\cdots S_{m_j}^{p*}S_{m_{j+1}}^{p}\cdots S_{m_{2j-1}}^{p} \\ &\times \mathrm{E}\Big[H_{k,n_1}\cdots H_{k,n_i}H_{k,n_{i+1}}^*\cdots H_{k,n_{2i-1}}^* \\ &\quad\times H_{k,m_1}^*\cdots H_{k,m_j}^*H_{k,m_{j+1}}\cdots H_{k,m_{2j-1}}\Big] \\ &\times g_{m_1+\cdots+m_j-m_{j+1}-\cdots-m_{2j-1}}^*(t_0-\tau) \\ &\times\int u_n(\tau')g_{n_1+\cdots+n_i-n_{i+1}-\cdots-n_{2i-1}}(t_0-\tau')d\tau'\end{aligned} \quad (15)$$

for $n=0,\cdots,N-1$. Therefore, it is possible to show that

$$u_n(t) = \sum_{i=i_{min}}^{i_{max}}\beta_{i,n}g_i^*(t_o-t) \quad (16)$$

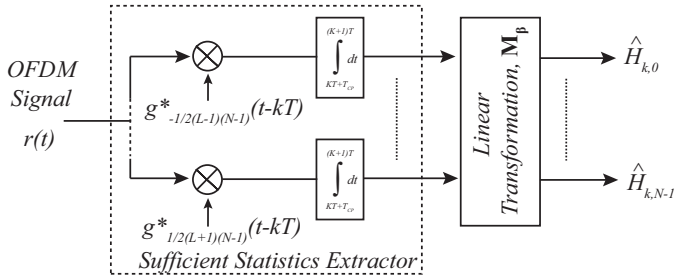

Fig. 3. Alternative structure of the proposed MMSE estimator.

where $i_{min} = -1/2(L-1)(N-1)$, $i_{max} = 1/2(L+1)(N-1)$ and $\beta_{i,n}$, $i = i_{min},\cdots,i_{max}$, n$=0,\cdots,N-1$, are constant coefficients that obey

$$\sum_{i=i_{min}}^{i_{max}}\beta_{i,n}\mathrm{E}\left[Y_{k,i}^pY_{k,m}^{p*}\right]+2N_0\beta_{m,n} = \mathrm{E}\left[H_{k,n}Y_{k,m}^{p*}\right] \quad (17)$$

for $m=-1/2(L-1)(N-1),\cdots,1/2(L+1)(N-1)$ and satisfy the integral equations in (13), where $Y_{k,i}^p$ are the received complex symbols given by (6) when the transmitted symbols are S_n^p. To see this use (16) in (15) and then use (15) and (14) in (13).

Equivalently, (17) can also be represented in matrix notation as

$$\mathbf{M}_\beta = \left\{\mathrm{E}\left[\mathbf{Y}_k^p\mathbf{Y}_k^{pH}\right]+2N_0\mathbf{I}\right\}^{-1}\mathrm{E}\left[\mathbf{Y}_k^{p*}\mathbf{H}_k^T\right] \quad (18)$$

where $\mathbf{Y}_k^p = \left[Y_{k,-1/2(L-1)(N-1)}^p,\cdots,Y_{k,1/2(L+1)(N-1)}^p\right]$ and $\mathbf{I}$ is the identity matrix.

The estimate of the channel frequency response in time slot k and subcarrier n is obtained by substituting the impulse response of the nth branch given by (16) in (11), i.e., $\hat{H}_{k,n} = \sum_{i_{min}}^{i_{max}}\beta_{i,n}R_{k,i}^p$, or in matrix notation as $\hat{\mathbf{H}}_k = \mathbf{M}_\beta^T\mathbf{R}_k^p$, where $\mathbf{R}_k^p$ represents the received symbols vector given that the vector of pilot symbols $\mathbf{S}^p$ was transmitted. Thus, the structure consisting of a set of linear filters can also be, alternatively, represented by a set of correlators matched to every possible frequency components of the nonlinearly distorted OFDM responsible for the extraction of the sufficient statistics of signal $r(t)$, i.e., no other statistic retrieved from the same signal can provide additional valuable information, followed by a linear transformation defined by coefficients $\beta_{i,n}$ given by (18) (see Figure 3).

Let us now focus on the derivation of matrix of

This article has been accepted for publication in a future issue of this journal, but has not been fully edited. Content may change prior to final publication. Citation information: DOI 10.1109/TCOMM.2014.2334619, IEEE Transactions on Communications

coefficients $\mathbf{M}_\beta$. The elements $\mathrm{E}\left[\mathbf{Y}_k^p \mathbf{Y}_k^{pH}\right]$ are given

$$\begin{aligned}\mathrm{E}\left[Y_{k,a}^p Y_{k,b}^{p*}\right] = &\sum_{i=1}^{(L+1)/2} \sum_{j=1}^{(L+1)/2} \frac{c_i c_j^*}{(T-T_{CP})^{(i+j-2)/2}} \\ &\times \sum_{n_i=0}^{N-1} \cdots \sum_{n_{2i-1}=0}^{N-1} \sum_{m_j=0}^{N-1} \cdots \sum_{m_{2j-1}=0}^{N-1} S_{n_1}^p \cdots S_{n_i}^p \\ &\times S_{n_{i+1}}^{p*} \cdots S_{n_{2i-1}}^{p*} S_{m_1}^{p*} \cdots S_{m_j}^{p*} S_{m_{j+1}}^{p} \cdots S_{m_{2j-1}}^{p} \\ &\times \mathrm{E}\Big[H_{k,n_1} \cdots H_{k,n_i} H_{k,n_{i+1}}^* \cdots H_{k,n_{2i-1}}^* \\ &\quad H_{k,m_1}^* \cdots H_{k,m_j}^* H_{k,m_{j+1}} \cdots H_{k,m_{2j-1}}\Big] \\ &\times \delta(a - n_1 - \cdots - n_i + n_{i+1} + \cdots + n_{2i-1}) \\ &\times \delta(b - m_1 - \cdots - m_j + m_{j+1} + \cdots + m_{2j-1})\end{aligned} \tag{19}$$

for $a, b = -1/2(L-1)(N-1), \cdots, 1/2(L+1)(N-1)$.

Similarly, elements $\mathrm{E}\left[\mathbf{Y}_k^{p*} \mathbf{H}_k^T\right]$ are given by

$$\begin{aligned}\mathrm{E}\left[Y_{k,a}^{p*} H_{k,n}\right] = &\sum_{i=1}^{(L+1)/2} \frac{c_i^*}{(T-T_{CP})^{(i-1)/2}} \\ &\times \sum_{n_i=0}^{N-1} \cdots \sum_{n_i=0}^{N-1} S_{n_1}^{p*} \cdots S_{n_i}^{p*} S_{n_{i+1}}^{p} \cdots S_{n_{2i-1}}^{p} \\ &\times \mathrm{E}\left[H_{k,n} H_{k,n_1}^* \cdots H_{k,n_i}^* H_{k,n_{i+1}} \cdots H_{k,n_{2i-1}}\right] \\ &\times \delta(a - n_1 - \cdots n_i + n_{i+1} + \cdots + n_{2i-1})\end{aligned} \tag{20}$$

To analytically derive (19) and (20) it is necessary to derive the expectation of the product of the complex Gaussian RVs $H_{k,n}$ present in (19) and (20). To do so, we refer to the Isserlis' theorem [18] which relates the expectation of products of jointly Gaussian RVs to products of pairs of these RV. This is now illustrated for two common fading models.

A. Rayleigh fading channel

The Isserlis' theorem states that the expectation of the product of m even zero-mean jointly Gaussian RVs, $\zeta_1 \cdots \zeta_m$, is equal to the sum of all distinct ways of partitioning the RVs into pairs, while for m odd it equals zero, irrespective of their mutual correlation, i.e.,

$$\mathrm{E}\left[\zeta_1 \zeta_2 \cdots \zeta_m\right] = \begin{cases} \sum \prod \mathrm{E}\left[\zeta_i \zeta_j\right], & m \text{ is even} \\ 0, & m \text{ is odd} \end{cases} \tag{21}$$

This yields $m! / \left[(m/2)! 2^{(m/2)}\right]$ terms in the sum, each being the product of $m/2$ covariances $\mathrm{E}\left[\zeta_i \zeta_j\right]$. From (19) and (20) we can also note that all expectations are in fact the product of m Gaussian RVs in which $m/2$ are complex conjugate. Therefore, the computation of the product of zero-mean jointly Gaussian RVs reduces to a sum of products of pairs.

From (5) and its corresponding channel transfer function it is possible to show that the three combinations of expectation of product of pairs in (21) reduce to $\mathrm{E}\left[H_{k,n_1} H_{k,n_2}\right] = 0$; $\mathrm{E}\left[H_{k,n_1}^* H_{k,n_2}^*\right] = 0$ and $\mathrm{E}\left[H_{k,n_1} H_{k,n_2}^*\right] = \mathrm{E}\left[|h_g|^2\right] \sum_{g=0}^{G-1} e^{-j\frac{2\pi t_g}{T}(n_1 - n_2)}$. Without loss of generality, we assume that the channel is normalized, i.e., $\mathrm{E}\left[|h_g|^2\right] = 1/G$.

B. Rician fading channel

Here, the frequency responses $H_{k,n}$ are considered to be non-zero mean complex Gaussian distributed. For m RVs $\psi_i = \zeta_i + \mu_i$, with means $\mu_1, \cdots, \mu_m$, where ζ_i is a zero-mean complex Gaussian distributed RV, and by expanding the expectation of the product of ψ_i it can be easily proven that it also reduces to a summation of expectations of zero-mean jointly Gaussian RVs affected by mean values μ_m. Thus, its computation also follows the procedure described for the Rayleigh fading case.

C. Extensions

In OFDM systems the subcarrier frequency spacing, Δf, is typically much smaller than the total bandwidth and as a result, the tolerable carrier frequency offset (CFO) becomes a very small fraction of the total bandwidth making it hard to synchronize the frequency. When CFO is present, orthogonality between subcarriers is lost, resulting in intercarrier interference (ICI) [3] and in a rotation of the received constellation that is not distinguishable from the random attenuation/rotation imposed by the multipath channel.

Consider now the complex envelope of the received OFDM signal affected by both frequency and phase offsets, respectively, δf and ϕ, given by

$$r'(t) = r(t) e^{j(2\pi \delta f t + \phi)} \tag{22}$$

We will now extend the MMSE CE described in Section III to take also into account these impairments. The new structure was found to be also the one represented in Figure 3. Yet, the expectation values $\mathrm{E}\left[\mathbf{Y}_k'^p \mathbf{Y}_k'^{pH}\right]$ and $\mathrm{E}\left[\mathbf{Y}_k'^{p*} \mathbf{H}_k'^{pT}\right]$ are now given

This article has been accepted for publication in a future issue of this journal, but has not been fully edited. Content may change prior to final publication. Citation information: DOI 10.1109/TCOMM.2014.2334619, IEEE Transactions on Communications

by

$$\begin{aligned}
\mathrm{E}\left[Y'^{p}_{k,a}Y'^{p*}_{k,b}\right] &= \sum_{i=1}^{(L+1)/2}\sum_{j=1}^{(L+1)/2}\frac{c_i c_j^*}{(T-T_{CP})^{(i+j-2)/2}} \\
&\times \sum_{n_i=0}^{N-1}\cdots\sum_{n_{2i-1}=0}^{N-1}\sum_{m_j=0}^{N-1}\cdots\sum_{m_{2j-1}=0}^{N-1} S^{p}_{n_1}\cdots S^{p}_{n_i} \\
&\times S^{p*}_{n_{i+1}}\cdots S^{p*}_{n_{2i-1}} S^{p*}_{m_1}\cdots S^{p*}_{m_j} S^{p}_{m_{j+1}}\cdots S^{p}_{m_{2j-1}} \\
&\times \mathrm{E}\Big[H^{p}_{k,n_1}\cdots H^{p}_{k,n_i} H^{p*}_{k,n_{i+1}}\cdots H^{p*}_{k,n_{2i-1}} \\
&\quad \times H^{p*}_{k,m_1}\cdots H^{p*}_{k,m_j} H^{p}_{k,m_{j+1}}\cdots H^{p}_{k,m_{2j-1}}\Big] \\
&\times \alpha_{a,n_1+\cdots+n_i-n_{i+1}-\cdots-n_{2i-1}} e^{j\gamma_{k,a,n_1+\cdots+n_i-n_{i+1}-\cdots-n_{2i-1}}} \\
&\times \alpha^*_{b,m_1+\cdots+m_j-m_{j+1}\cdots-m_{2j-1}} \\
&\times e^{-j\gamma_{k,b,m_1+\cdots+m_j-m_{j+1}-\cdots-m_{2j-1}}}
\end{aligned} \tag{23}$$

and

$$\begin{aligned}
\mathrm{E}\left[Y'^{p*}_{k,a}H_{k,n}\right] &= \sum_{i=1}^{(L+1)/2}\frac{c_i^*}{(T-T_{CP})^{(i-1)/2}} \\
&\times \sum_{n_i=0}^{N-1}\cdots\sum_{n_i=0}^{N-1} S^{p*}_{n_1}\cdots S^{p*}_{n_i} S^{p}_{n_{i+1}}\cdots S^{p}_{n_{2i-1}} \\
&\times \mathrm{E}\left[H_{k,n}H^{p*}_{k,n_1}\cdots H^{p*}_{k,n_i} H^{p}_{k,n_{i+1}}\cdots H^{p}_{k,n_{2i-1}}\right] \\
&\times \alpha_{a,n_1+\cdots+n_i-n_{i+1}-\cdots-n_{2i-1}} e^{j\gamma_{k,a,n_1+\cdots+n_i-n_{i+1}-\cdots-n_{2i-1}}}
\end{aligned} \tag{24}$$

for $a, b = -1/2(L-1)(N-1), \cdots, 1/2(L+1)(N-1)$ and where the attenuation and the time-varying phase shift factors are given, respectively, by

$$\alpha_{x,n_l} = \mathrm{sinc}\left[(n_l - x) + \delta f(T - T_{CP})\right] \tag{25}$$

$$\gamma_{k,x,n_l} = \pi(n_l - x) + \pi\delta f[(2k+1)T + T_{CP}] + \phi \tag{26}$$

As it can be seen from (23) and (24), the expectation values of the joint carrier frequency/phase offsets and MMSE CE reduces again to the computation of the expectation value of the product of complex Gaussian RVs. Therefore, its analytical computation follows the procedure described in sections III-A and III-B. Similarly, the linear transformation given by (18) can also be derived using (23) and (24). Since the CFO estimation topic is out of the scope of this work, here we consider that the channel estimator structure knows the CFO value.

D. Considerations on the estimator complexity

The computation of the MMSE estimator can be in fact quite complex. Nevertheless, if the nonlinear channel is assumed to be static and the statistical properties of the fading process do not change frequently over time, the estimator only needs to compute the linear transformation once and the estimation process reduces to a multiplication between a $[L(N+1)+1] \times N$ size matrix and a $[L(N+1)+1] \times 1$ size vector. This assumption is considered to be realistic since 1) the nonlinear channel given by the electrical-optical converter does not change over time, and 2) although the fading channel may vary over time, in typical indoor WiFi scenarios, its statistical properties do not.

Alternatively to the analytical computation, and by knowing that the mean of the product of Gaussian RV tend to its expected value, equations 23 and 24 can be computed and approximated using Monte-Carlo techniques. Preliminary results have shown that with only a few hundreds of fading channel computations it is possible to obtain a good approximation of the MMSE CE linear transformation matrix with a drastically reduced computation time.

IV. Case Study: WiFi over Fiber

In this section we assess the performance of the CE by considering an uplink RoF system that conveys OFDM signals with parameters in accordance with the IEEE802.11g/n standard [5].

A. System model

We consider the typical IM/DD uplink RoF transmission in Figure 1. The nonlinear element in the model is given by the MZM transfer function which is well modeled by Taylor series expansion. Additionally, the following noise sources are also considered: the antenna at the BS given by an equivalent antenna temperature; the relative intensity noise (RIN) from the LASER; and both shot and thermal noises at the PIN photodiode, that are assumed to follow collectively a Gaussian distribution. The optical fiber is considered to act only as an attenuation channel. This assumption is valid for double side band (DSB) for fiber lengths up to tens of kilometers or SSB, the latter avoiding the beating between the two bands. Nonlinear fiber effects are also masked by other impairments such as electro-optic converter nonlinear distortion and

This article has been accepted for publication in a future issue of this journal, but has not been fully edited. Content may change prior to final publication. Citation information: DOI 10.1109/TCOMM.2014.2334619, IEEE Transactions on Communications

noise, for relatively low optical powers (< 0 dBm) and fiber distances of typical RoF scenarios (e.g. [19]). Moreover, the impact of a CFO between the transmitted and receiver is also addressed. Additional impairments such as MZM chirp, IQ imbalances and nonlinear effects of the fiber fall outside of the scope of this study. The MZM has an input-output characteristic given by

$$P_{out}(t) = P_{CW}\cos^2\left\{\frac{\pi}{2V_\pi}[x(t)+V_b]\right\} \qquad (27)$$

where P_{CW} is the optical power of the LASER, $x(t)$ is the AC component of the voltage signal, V_b is the bias DC voltage applied and V_π is the voltage required to induce a π phase shift in the optical signal. Note that in our scenario the signal $x(t)$ represents the faded OFDM RF signal (see Figure 2). The nonlinear operating point can be defined by the modulation index of $x(t)$ which is given by the ratio $m_i = \sigma_x/(0.5V_\pi)$, where σ represents the standard deviation. Note that the modulation index is imposed by the MZM driver represented in Figure 1 which acts as an automatic gain controller (AGC). Since it is placed at the BS, its size and power consumption are not a major constraint, allowing us to simplify our analysis and consider that its compression point is relatively high and, thus, its transfer function is linear.

In order to operate in a quasi-linear region, V_b is set to $V_\pi/2$. After the fiber, a photocurrent proportional to the incident optical power affected by a responsivity is generated at the photodiode. This responsivity is set to $\mathcal{R} = 1$ A/W.

Since we are focusing on an uplink scenario and on post compensation techniques for both channel estimation and symbol detection, we assess the performance of the MMSE CE by comparing it with the one obtained by the widely used ZF based and by the ideal perfect estimation. For the symbol detection, we consider two different equalizer structures: the one-tap equalizer and an iterative structure based on ML decision rule given by (8) and (9), respectively. Due to its high computational cost, the iterative algorithm only evaluates a restricted group of data vectors that differ by one bit from the last estimate vector. Then, the process is repeated iteratively in order to refine the estimate of the transmitted symbols vector. The starting point of the algorithm, i.e., iteration 'zero', is provided by a conventional OFDM receiver followed by the one-tap equalizer. It is also important to note that the algorithm typically converges to a local optimum solution rather than the optimal one [16], [20]. While the "true" ML detection has an associated complexity of order $O(M^N)$, the one of the iterative ML algorithm is $O(lNlog_2(M))$, where l is the number of iterations used.

Results are obtained by first obtaining a channel estimative using pilots defined in the standard. In this first stage, the OFDM pilot symbol is affected by a randomly generated multipath channel IR. Subsequently, the faded OFDM symbol is corrupted by noise from the BS antenna and then distorted by the nonlinearity. Finally, after being corrupted again with noise at the photodiode, the OFDM pilot symbol is used to estimate the frequency response of the multipath channel. In the end, the overall estimate is given by averaging the estimates for each subchannel index.

In the second stage, associated with the transmission of data symbols for detection, an OFDM signal conveying uniformly random generated complex symbols is considered. Then, the signal passes through the RoF system previously described in stage one; at the OFDM receiver equalizer an estimation of the transmitted complex symbols is obtained by using the channel estimate. As typically occurs in practice, it is considered that the multipath channel is constant over both stages.

The PDP profile associated with the multipath channel was set to $\Omega(\tau) \propto e^{-\tau/\tau_{rms}}$, where τ_{rms} is the RMS delay spread set to 100 ns. Note that the PDP is normalized and so the average received power equals to one. The fading channel is set to a 6 tap TDL channel, Rician distributed (typically used for indoor scenarios) with a Rician K-factor of 10 dB. A complex automatic gain control (CAGC) was computed and applied to all received complex symbols in order to correctly demodulate amplitude modulations like 16-QAM.

A sampling frequency high enough to accommodate IMPs generated up to the $15th$ order is considered. The linear transformation of the CE structure was obtained for IMPs up to the $7th$ order due to its high computation complexity associated with higher orders.

For our simulations, we consider the transmission of OFDM signals conveying 16-QAM symbols as defined in the standard. Each OFDM symbol is

This article has been accepted for publication in a future issue of this journal, but has not been fully edited. Content may change prior to final publication. Citation information: DOI 10.1109/TCOMM.2014.2334619, IEEE Transactions on Communications

created using the IFFT algorithm with 64 points with a period of $3.2\,\mu$s and cyclic prefix of $0.8\,\mu$s. The number of subcarriers used is 52 from which 48 are for data, four for pilots and the remaining eight are null-valued. The pilot subcarriers can be used to help synchronization and to allow a coherent detection robust against CFO and phase noise. Yet, since we consider a block type estimation procedure and that the channel is invariant over both channel estimation and equalization stages, these four pilots are not taken into consideration. Also, forward error correction coding and scramblers defined by the standard are not considered since we focus on the receiver performance over raw data. Additionally, with respect to the analog-to-digital converter (ADC) receiver front-end, we have conducted several numerical simulations and concluded that a quantization resolution of 7 bit enforces a minimum SQNR of 34.51 dB and, in these conditions, no impact on the overall performance is seen. These results are in agreement with the ones reported in the literature [15] and are considerable higher than the SNR values considered when modeling the BS antenna and the receiver noise sources (due to RIN, shot and thermal noises). Furthermore, the SQNR values obtained are also consistent with the minimum SNR value of 20 dB necessary for a reliable WiFi transmission [21]. Hence, we can conclude that for ADC/DAC resolutions higher than 6 bits, the quantization noise is negligible compared to the other impairments and has no impact on the considered RoF uplink system. Similarly, its cascaded effect is also considered to be negligible for the system under study.

B. Simulation results

We use as performance metrics the bit error rate (BER) and the total degradation (TD) defined at the output of the MZM as [22]

$$\text{TD[dB]} = \left[\left(\frac{E_b}{N_0}\right)_{NL} - \left(\frac{E_b}{N_0}\right)_{L}\right] + \text{OBO} \quad (28)$$

where $(E_b/N_0)_{NL}$ is the required SNR per bit at the input of the threshold detector to obtain a fixed BER for a given OBO value, $(E_b/N_0)_L$ is the required SNR per bit in decibels to obtain the same fixed BER in absence of nonlinearity, and OBO is the output back-off. In other words, it is the sum of the OBO and the increment in the SNR to achieve a given BER with respect to the case of a linear channel. The OBO parameter identifies the operating point and is defined as the ratio between the maximum output power that a nonlinear element can exhibit and the average output power of a given signal. Thus, its value is inversely related with the degree of nonlinear strength.

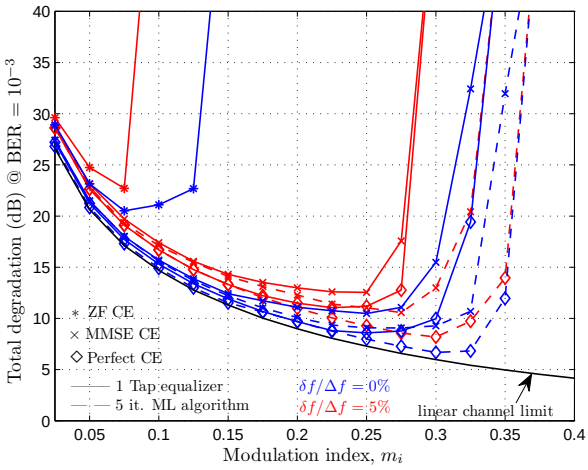

Fig. 4. TD vs. m_i considering ZF, MMSE and perfect CEs and both the one-tap equalizer and the 5 iterations ML algorithm for a target BER of 10^{-3}. Results for normalized CFO values 0% and 5%.

Figure 4 shows the TD of the system for a BER target of 10^{-3} considering ZF, MMSE and perfect CEs, as well as both one-tap and five iterations ML algorithm equalizers for normalized CFOs of 0% and 5% scenarios. A limit denoted as "linear channel" is also plotted to indicate the degradation value if, instead of the MZM, a linear channel was considered. Results show that there is a considerable gain when using the MMSE CE instead of a simple ZF, albeit not matching the perfect estimation curves. Let us first consider the 0% CFO case. Results show minimum TD values of 10.5 dB and 8.6 dB for the MMSE and perfect CE followed by one-tap equalizer, respectively, and 9 dB and 6.7 dB when followed by the 5 iterations ML algorithm equalizer. In other words, the MMSE CE structure shows degradation values relative to the perfect estimator of 1.9 dB and 2.3 dB for one-tap and iterative ML equalizers, respectively. The ZF estimator presents a minimum TD 13.8 dB higher than the MMSE estimator. With respect to the 5% normalized CFO case, the MMSE CE structure shows a degradation relative to the perfect estimation of 1.5 dB and 2.3 dB for one-tap and 5 iterations ML algorithm equalizers. These

This article has been accepted for publication in a future issue of this journal, but has not been fully edited. Content may change prior to final publication. Citation information: DOI 10.1109/TCOMM.2014.2334619, IEEE Transactions on Communications

TABLE I
LINK GAIN MARGINS AND OPTICAL FIBER LENGTHS, BER = 10^{-3}

		MMSE CE→ZF CE	MMSE CE→Perfect CE
No CFO	1 Tap Eq.	11.5 dB [28.8 Km]	−1.9 dB [−4.8 Km]
	5 it. ML	13.8 dB [34.5 Km]	−2.3 dB [−5.8 Km]
5% CFO	1 Tap Eq.	10.2 dB [25.5 Km]	−1.5 dB [−3.8 Km]
	5 it. ML	12.2 dB [30.5 Km]	−2.3 dB [−5.8 Km]

results suggest a small relative improvement in terms of total degradation when using the MMSE CE/one-tap equalizer in a CFO scenario. Moreover, the ZF estimator presents a minimum TD 12.2 dB higher than the MMSE estimator. Thus, we conclude that link gain of that same amount is achieved. This margin can be used to relax the receiver's noise level or to decrease the signal power by increasing the optical link path in up to 30.5 km (considering an optical loss of 0.2 dB/km)[3]. Table I summarizes the maximum link gains and their equivalent in terms of optical fiber lengths for the transmission cases depicted in Figure 4. The negative values for the MMSE with respect to the perfect estimator represent losses.

To perform a BER analysis, we set the overall noise level at the photodiode to 3.5×10^{-23} A^2/Hz and the incident optical power at the input of the photodiode to -19 dBm[4]. The noise at the photodiode is considered to be WGN within the signal's band. Besides the ideal antenna model at the BS, we also consider a scenario where an equivalent antenna temperature of 290 K is present, resulting in a noise PSD level of -114 dBm/MHz. Thus, for an acceptable SNR of 20 dB necessary for a reliable transmission [21], the minimum received PSD at the BS antenna is -94 dBm/MHz.

Figure 5 shows the BER as function of the modulation index for both one-tap equalizer and the five iterations ML algorithm acting as equalizer and for two SNR_{AN} levels at the BS antenna. Moreover, results for the ZF, MMSE and perfect CEs are also depicted. It can be seen that a significant improvement is reported when using the MMSE CE for both antenna noise levels. Furthermore, a performance improvement is also obtained if a 5 iterations ML algorithm is used as equalizer, instead of the conventional one-tap. Regarding the non-ideal antenna case, the MMSE CE is no longer optimum in the MSE sense. Nevertheless, it is still capable to process the distorted signal. In conclusion, for a given receiver's noise level and by post compensation of the signal, a decrease of the raw data BER of several orders of magnitude is reported. This allows for both the increase of the useful data rate and a higher dynamic range of the input signal.

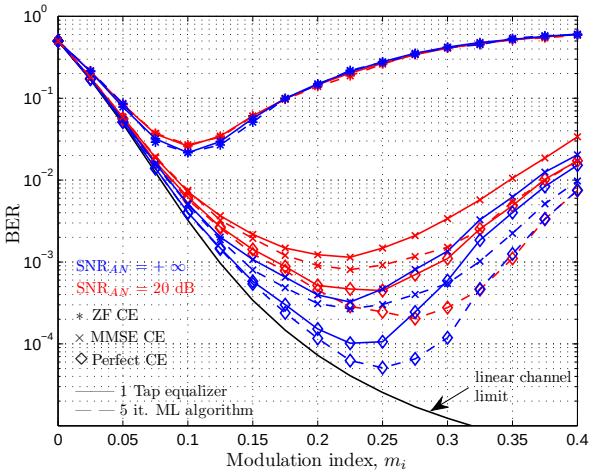

Fig. 5. BER vs. m_i considering the ZF, MMSE and perfect CEs and both the one-tap equalizer and the 5 iterations ML algorithm. Results for SNR antenna levels $\text{SNR}_{\text{AN}} = +\infty$ and $\text{SNR}_{\text{AN}} = 20$ dB.

V. CONCLUSIONS

In this paper, a new linear MMSE based CE for nonlinearly distorted faded OFDM signals corrupted by AWGN has been analytically derived. The key element of novelty relates to the fact that this estimator, in contrast to other CEs, incorporates both the effect of linear and nonlinear distortion, in the estimation process. We have demonstrated that it is given by a set of N linear filters or, equivalently, a set of correlators matched to every possible frequency components followed by a linear transformation so that it can be immediately incorporated into a standard OFDM receiver. We have also demonstrated that a structure suitable for signals that also suffer of CFO can be obtained without significant changes to the original one.

The performance of the MMSE CE was evaluated in a specific RoF uplink scenario that conveys an OFDM signal based on the WiFi standard. Results have showed that the ZF CE is severally affected by

[3]Preliminary results for high time consuming simulations considering a BER target of 10^{-4} and a higher number of iterations of the ML algorithm have shown that higher gain margins can be achieved.

[4]To avoid very low BER that would take too much time to simulate, a low optical power at the input of the photodiode is considered.

This article has been accepted for publication in a future issue of this journal, but has not been fully edited. Content may change prior to final publication. Citation information: DOI 10.1109/TCOMM.2014.2334619, IEEE Transactions on Communications

IMD. On the other hand, results have showed that the MMSE CE can be used to estimate the frequency response of the multipath channel even in the presence of antenna noise and CFO. In fact, results have showed relatively low degradation values which are close to the ones for perfect estimation.

Regarding the iterative ML algorithm when acting as an equalizer, we have reported performance improvements for both MMSE and perfect estimators, comparatively to the one-tap equalizer. Results for a BER of 10^{-3} indicate that with the proposed algorithms it is possible to add up to 34.5 km of optical fiber and still obtain the same TD as the conventional structures. In conclusion, this case study shows the feasibility to process the distorted OFDM received signal in order to improve performance without using pre-distortion techniques thereby reducing the complexity of the wireless devices. Additionally, results show that by using the proposed post compensation techniques, it is possible to relax the noise requirements of the receiver or, similarly, allow a higher attenuation of the optical link equivalent to several kilometers in order to obtain the same degradation as the conventional structures. Also, for a given receiver noise level, a decrease of the raw data BER in several orders of magnitude was reported. This allows both an increase of the useful data rate and a higher dynamic range of the signal. Finally, we conclude that the proposed CEs and receivers are therefore suitable for improving the performance of the uplink of fiber supported wireless systems.

REFERENCES

[1] "Mobile traffic forecasts 2010-2020," UMTS Forum, Tech. Rep., January 2011.

[2] L. K. Vanston and R. Hodges, "Forecasts for the US telecommunications network," *Telektronnik*, vol. 104, no. 3/4, pp. 18–28, 2008.

[3] R. Prasad, *OFDM for wireless communications systems*. Artech House Publishers, 2004.

[4] IEEE 802.11g-2003 Standard, "Local and metropolitan area networks – Specific requirements – Part 11: Wireless LAN medium access control (MAC) and physical layer (PHY) specification – Amendment 4: Further high data rate extension in the 2.4 GHz band," June 2003.

[5] IEEE 802.11n-2009 Standard, "Local and metropolitan area networks – Specific requirements – Part 11: Wireless LAN medium access control (MAC) and physical layer (PHY) specification: Enhancements for higher throughput," October 2009.

[6] IEEE 802.16e-2005 Standard, "Local and metropolitan area networks – Part 16: Air interface for fixed and mobile broadband wireless access systems – Amendment 2: Physical and medium access control layers for combined fixed and mobile operation in licensed bands and corrigendum 1," February 2006.

[7] C. Lim, A. Nirmalathas, M. Bakaul, P. Gamage, K. Lee, Y. Yang, D. Novak, and R. Waterhouse, "Fiber-wireless networks and subsystem technologies," *Lightwave Technology, Journal of*, vol. 28, no. 4, pp. 390–405, 2010.

[8] D. Lowe and X. Huang, "Adaptive low-complexity mmse channel estimation for ofdm," in *Communications and Information Technologies, 2006. ISCIT'06. International Symposium on*. IEEE, 2006, pp. 638–643.

[9] M. Morelli and U. Mengali, "A comparison of pilot-aided channel estimation methods for ofdm systems," *Signal Processing, IEEE Transactions on*, vol. 49, no. 12, pp. 3065–3073, 2001.

[10] J. Van de Beek, O. Edfors, M. Sandell, S. Wilson, and P. Borjesson, "On channel estimation in OFDM systems," in *Vehicular Technology Conference, 1995 IEEE 45th*, vol. 2. IEEE, 1995, pp. 815–819.

[11] M. Ozdemir and H. Arslan, "Channel estimation for wireless OFDM systems," *Communications Surveys & Tutorials, IEEE*, vol. 9, no. 2, pp. 18–48, 2007.

[12] T. Hwang, C. Yang, G. Wu, S. Li, and G. Ye Li, "Ofdm and its wireless applications: a survey," *Vehicular Technology, IEEE Transactions on*, vol. 58, no. 4, pp. 1673–1694, 2009.

[13] S. Benedetto and E. Biglieri, *Principles of digital transmission: with wireless applications*. Plenum Pub Corp, 1999.

[14] D. Tse and P. Viswanath, *Fundamentals of wireless communication*. Cambridge Univ Pr, 2005.

[15] Y. Cho, J. Kim, W. Yang, and C. Kang, *MIMO-OFDM wireless communications with MATLAB*. Wiley, 2010.

[16] J. Oliveira, M. Rodrigues, and H. Salgado, "Optimum receivers for non-linear distortion compensation of ofdm signals in fiber supported wireless applications," in *Microwave Photonics, 2007 IEEE International Topical Meeting on*, 2007, pp. 120–123.

[17] R. Weinstock, *Calculus of variations: with applications to physics and engineering*. Dover Pubns, 1974.

[18] L. Isserlis, "On a formula for the product-moment coefficient of any order of a normal frequency distribution in any number of variables," *Biometrika*, vol. 12, no. 1/2, pp. 134–139, 1918.

[19] G. Smith, D. Novak, and Z. Ahmed, "Overcoming chromatic-dispersion effects in fiber-wireless systems incorporating external modulators," *IEEE Transactions on Microwave Theory and Techniques*, vol. 45, no. 8, pp. 1410–1415, 1997.

[20] H. Nishijima, M. Okada, and S. Komaki, "A sub-optimum nonlinear distortion compensation scheme fororthogonal multicarrier modulation systems," *7th IEEE International Symposium on Personal, Indoor and Mobile Radio Communications*, 1996.

[21] W. N. Corporation, "Product specifications of DNMA-92, an IEEE802.11a/b/g/n Mini-PCI module, version 1.6," April 2009.

[22] G. Santella and F. Mazzenga, "A hybrid analytical-simulation procedure for performance evaluation in M-QAM-OFDM schemes in presence of nonlinear distortions," *IEEE Transactions on Vehicular Technology*, vol. 47, pp. 142–151, 1998.

This article has been accepted for publication in a future issue of this journal, but has not been fully edited. Content may change prior to final publication. Citation information: DOI 10.1109/TCOMM.2014.2334619, IEEE Transactions on Communications

João M. B. Oliveira graduated and obtained his PhD degree both in Electrical and Computer Engineering from the Faculty of Engineering of the University of Porto, Portugal, in 2005 and 2012, respectively.

He is currently a Project Engineering Manager at Synopsys Inc., Portugal. He was previously with the Optical and Electronic Technologies group at INESC TEC, Portugal, as a researcher in the FP7 EU project DAPHNE (Developing Photonic Aircraft Networks) and FP6 EU project UROOF (Photonics Components for Ultra-Wideband Radio over Optical Fibre). He has published several papers in top-conferences and journals of topics such as microwave photonics, electronics and signal processing.

His research interests include: optical communications systems, digital signal processing, advanced modulation formats, radio-over-fiber systems, RF electronics and electronic design.

Henrique M. Salgado graduated in Applied Physics (Optics and Electronics) from the University of Porto in 1985 and received the PhD degree in Electronic Engineering and Computer Systems from University of Wales in 1993. He joined the Department of Electrical Engineering and Computers of the University of Porto in 1999 as an Invited Assistant Professor and in 2003 he became Associate Professor. Since 1995 that he heads the Optical Communications and Microwaves Group at INESC Porto, being responsible for several national and internationally funded (EU) research projects. From 1997 - 1999 he was Research Fellow at the Department of Electrical and Electronic Engineering of the University College London, UK and previously Research Assistant at the School of Electronic Engineering and Computer Systems, Bangor, UK. He is the author and coauthor of numerous international publications in the field of optical fibre communications and microwaves. His current research interests include: radio-over-fiber technology and microwave photonics, digital equalization in coherent optical systems, alloptical networks, modeling of nonlinearities and design of compact multiband antennas. He is a member of the Photonics and Communications societies of the IEEE.

Miguel R. D. Rodrigues (S'98-A'02-M'03) received the Licenciatura degree in Electrical Engineering from the University of Porto, Portugal in 1998 and the Ph.D. degree in Electronic and Electrical Engineering from University College London, U.K. in 2002.

He is currently a Senior Lecturer with the Department of Electronic and Electrical Engineering, University College London, UK. He was previously with the Department of Computer Science, University of Porto, Portugal, rising through the ranks from Assistant to Associate Professor, where he also led the Information Theory and Communications Research Group at Instituto de Telecomunicações - Porto. He has held postdoctoral or visiting appointments with various Institutions worldwide including University College London, Cambridge University, Princeton University, and Duke University in the period 2003-2013.

His research work, which lies in the general areas of information theory, communications and signal processing, has led to over 100 papers in journals and conferences to date. Dr. Rodrigues was also honored by the IEEE Communications and Information Theory Societies Joint Paper Award in 2011 for his work on Wireless Information-Theoretic Security (joint with M. Bloch, J. Barros and S. M. McLaughlin). Dr. Rodrigues currently serves as an Associate Editor to the IEEE Communications Letters.